TRANSIENT ASPECTS OF TRANSITION RADIATION*

BY

E. OTT AND J. SHMOYS

Polytechnic Institute of Brooklyn

I. Introduction. When a charged particle moving at uniform velocity crosses a boundary between two media with different electrical properties, a pulse of electromagnetic energy is emitted. This phenomenon is basically unlike either bremsstrahlung or the Cerenkov effect in that the charge will radiate even though it does not accelerate or move faster than the phase velocity of light in the medium.

Various theoretical [1] and experimental [2] aspects of transition radiation have recently been the subject of extensive study. It has been proposed that the effect might be useful in the generation of microwave power and as a diagnostic tool for the study of metals and plasmas.

It is clear that the effect is fundamentally a transient process. It is, therefore surprising that the transient character of the fields has hardly received notice. Previous investigators have concentrated on determining the frequency spectrum of the radiation fields. We, on the other hand, will deal directly with the problem of finding the fields as a function of time.[1]

In order to illustrate the essential characteristics of the processes involved, a specific problem will be considered. For the problem selected an exact closed form solution is obtained in a form amenable to physical interpretation. It is found that before the time of impact the entire field may be represented in terms of an image picture, which is a generalization of the static case. Even after impact the image picture remains valid, but only in certain regions of space. At impact, a sudden burst of energy is liberated. This energy then propagates outward from the impact point in a manner to be discussed later. It is to be expected that the solution of the present problem will aid in the understanding of transition radiation in more complicated configurations, for which no closed form solution is available.

The method used to evaluate the transient is patterned after that given by Felsen [3]. A representation of the solution in terms of Fourier integrals will be obtained; these will then be reduced to such a form that they can be evaluated by inspection.

II. The problem. We consider the situation in which the regions $z < 0$ and $z > 0$ are occupied by two different nondispersive media. The dielectric constant ϵ' and magnetic permittivity μ' are given by[2]

$$\epsilon' = \epsilon_\pm \quad \text{and} \quad \mu' = \mu_\pm \ .$$

The problem is that of determining the fields due to the charge density

$$n(\mathbf{r}, t) = Q\ \delta(x)\ \delta(z - k(t)) - Q\ \delta(x)\ \delta(z + vT + \delta z) \tag{1}$$

*Received September 12, 1966; revised manuscript received December 7, 1966.

[1]It has recently come to the attention of the authors that J. Cohen and R. M. Lewis have been investigating the transient transition radiation problem. Their work and ours, however, are very different in both viewpoint and content.

[2]In terms of notation the statement: "$\mu' = \mu_+$ for $z > 0$ and $\mu' = \mu_-$ for $z < 0$" is written as $\mu' = \mu_\pm$. This notation will be used throughout.

where T, δT and δz are positive and $k(t) = vt$ for $t \geq -T$ and $k(t) = -vT - \delta z$ for $t \leq -T - \delta T$. Furthermore we assume that $k(t)$ is monotonic and that dk/dt is continuous with $dk/dt = 0$ at $t = -T - \delta T$. The first term in (1) is representative of a moving line charge of strength Q, which starts moving from its rest position, $z = -vT - \delta z$, at the time $t = -T - \delta T$. By the time $t = -T$ the moving charge has accelerated to the velocity v, which it maintains for all time thereafter, $t \geq -T$. The second term in (1) is representative of a stationary line charge of strength $-Q$, whose presence conveniently assures that the charge density is zero for all time $t \leq -T - \delta T$. In (1), $\delta(x)$ stands for the Dirac delta function. The two dimensional problem thus formulated is illustrated in Fig. 1.

We seek the solution to Maxwell's equations with the source $n(\mathbf{r}, t)$ which satisfies the jump conditions at $z = 0$ and the initial conditions at $t = -T - \delta T$. Maxwell's equations, valid for $t \geq -T - \delta T$, are

$$\nabla \times \mathbf{E}(\mathbf{r}, t) = -\mu_\pm \frac{\partial \mathbf{H}(\mathbf{r}, t)}{\partial t}, \tag{2}$$

$$\nabla \times \mathbf{H}(\mathbf{r}, t) = \epsilon_\pm \frac{\partial \mathbf{E}(\mathbf{r}, t)}{\partial t} + \mathbf{J}(\mathbf{r}, t) \tag{3}$$

where $\mathbf{J}(\mathbf{r}, t) = Q\delta(x)\delta(t - g(z))\mathbf{z}_0$ and $t = g(z)$ is the inverse of $z = k(t)$. We will use $\mathbf{x}_0$, $\mathbf{y}_0$, $\mathbf{z}_0$ to denote unit vectors in the directions of the corresponding axes. The jump conditions are that $\mathbf{H}(\mathbf{r}, t) \times \mathbf{z}_0$ and $\mathbf{E}(\mathbf{r}, t) \times \mathbf{z}_0$ are continuous across $z = 0$. The initial conditions are that $\mathbf{H}(\mathbf{r}, -T - \delta T) = 0$ and $\mathbf{E}(\mathbf{r}, -T - \delta T) = 0$. Since $\mathbf{J}$ is in the $\mathbf{z}_0$ direction

$$\mathbf{H} = H\mathbf{y}_0, \tag{5}$$

$$\mathbf{E} = E_z\mathbf{z}_0 + E_x\mathbf{x}_0 . \tag{6}$$

The problem can be reduced to a scalar problem in the single variable $F(\mathbf{r}, t)$, defined by

$$\mathbf{H} = \mathbf{y}_0(\partial F/\partial t), \tag{7}$$

so that at points other than $x = 0$,

$$\mathbf{E} = \frac{1}{\epsilon_\pm} \nabla \times (\mathbf{y}_0 F). \tag{8}$$

III. Formal solution. We now apply a Fourier transform in time to all the field quantities

$$\mathbf{E}(\mathbf{r}, t) = \frac{1}{2\pi} \int_{-\infty}^{+\infty} \exp(-i\omega t)\mathbf{e}(z, x, \omega)\, d\omega, \tag{9}$$

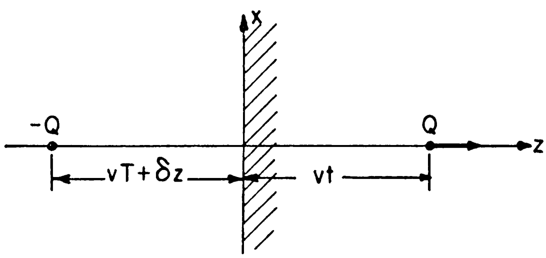

Fig. 1. The problem ($t > 0$).

$$H(\mathbf{r}, t) = \frac{1}{2\pi} \int_{-\infty}^{+\infty} \exp(-i\omega t) h(z, x, \omega)\, d\omega, \tag{10}$$

$$F(\mathbf{r}, t) = \frac{1}{2\pi} \int_{-\infty}^{+\infty} \exp(-i\omega t) f(z, x, \omega)\, d\omega. \tag{11}$$

From (2) and (3) (with $k_\pm^2 = \omega^2 \mu_\pm \epsilon_\pm$) we get

$$(\nabla^2 + k_\pm^2) f = \frac{Q}{i\omega} \exp(i\omega g(z)) \frac{\partial}{\partial x} \delta(x) u(z + vT + \delta z), \tag{12}$$

where $u(z)$ is the unit step. Introducing Fourier transforms in x

$$\mathbf{e}(z, x, \omega) = \frac{1}{2\pi} \int_{-\infty}^{+\infty} \exp(i\eta x) \mathbf{e}'(z, \eta, \omega)\, d\eta, \tag{13}$$

$$h(z, x, \omega) = \frac{1}{2\pi} \int_{-\infty}^{+\infty} \exp(i\eta x) h'(z, \eta, \omega)\, d\eta, \tag{14}$$

$$f(z, x, \omega) = \frac{1}{2\pi} \int_{-\infty}^{+\infty} \exp(i\eta x) f'(z, \eta, \omega)\, d\eta. \tag{15}$$

Utilizing the above, the following problem for $f'(z, \eta, x)$ results

$$\begin{aligned} [d^2/dz^2 + \alpha_\pm^2] f' &= 0, \qquad z \le -\delta z - vT \\ &= -\frac{Q\eta}{\omega} \exp(i\omega g(z)), \qquad -\delta z - vT \le z \le -vT \\ &= -\frac{Q\eta}{\omega} \exp(i\gamma z), \qquad -vT \le z, \end{aligned} \tag{16}$$

where

$$\alpha_\pm^2 = k_\pm^2 - \eta^2,$$

$$\gamma = \frac{\omega}{v}.$$

The jump conditions are that f' and $(\epsilon_\pm)^{-1}\, df'/dz$ are continuous across $z = 0$. In addition, since the fields are initially zero, we must require that the solution to (12) satisfies a radiation condition. The solution for f' satisfying (16) and the radiation condition is

$$f' = A_1 \exp(-i\alpha_- z), \qquad z \le -vT - \delta z, \tag{17a}$$

$$\begin{aligned} &= -\frac{Q\eta}{\omega} \int_{-\delta z}^{0} \frac{\exp\{i\alpha_- |z + vT - \xi| + i\omega g(\xi - vT)\}}{2i\alpha_-}\, d\xi \\ &\quad + A_2 \exp(-i\alpha_- z) + A_3 \exp(i\alpha_- z), \qquad -vT \ge z \ge -vT - \delta z, \end{aligned} \tag{17b}$$

$$= -\frac{Q\eta}{\omega} \frac{\exp(i\gamma z)}{\alpha_-^2 - \gamma^2} + A_4 \exp(-i\alpha_- z) + A_5 \exp(i\alpha_- z), \qquad 0 \ge z \ge -vT, \tag{17c}$$

$$= -\frac{Q\eta}{\omega} \frac{\exp(i\gamma z)}{\alpha_+^2 - \gamma^2} + A_6 \exp(i\alpha_+ z), \qquad z \ge 0, \tag{17d}$$

and the top Riemann sheet of $\alpha_\pm$ is defined so that $\operatorname{Im} \alpha_\pm \ge 0$ on the integration path in Eq. (15). The coefficients A_1, A_2, A_3, A_4, A_5, and A_6 are determined from the jump conditions at $z = 0$ and the conditions that f' and df'/dz are continuous at $z = -vT$ and $z = -vT - \delta z$.

In order to simplify the problem, we let $T \to +\infty$. Before taking the limit we add a small amount of loss to the medium in $z < 0$. Thus Im $\alpha_- > 0$ and the term $\exp(i\alpha_- vT) \to 0$ as $T \to +\infty$. Eqs. (17) reduce to

$$f' = -\frac{\eta Q}{\omega} \cdot \frac{\exp(i\gamma z)}{\alpha_\pm^2 - \gamma^2} + A_\pm \exp(i\alpha_\pm |z|) \tag{17'}$$

where $A_+ = \mathrm{Lim}_{T\to+\infty} A_6$ and $A_- = \mathrm{Lim}_{T\to+\infty} A_4$. The coefficients A_+ and A_- are given by

$$A_- = -\frac{\eta Q}{\omega}\left[\frac{1}{\alpha_+ + \gamma} - \frac{\alpha_+ - \epsilon\gamma}{\alpha_-^2 - \gamma^2}\right] \div [\alpha_+ + \epsilon\alpha_-], \tag{18}$$

$$A_+ = -\frac{\eta Q}{\omega}\epsilon\left[\frac{1}{\alpha_- - \gamma} - \frac{\alpha_- + \gamma/\epsilon}{\alpha_+^2 - \gamma^2}\right] \div [\alpha_+ + \epsilon\alpha_-] \tag{19}$$

where $\epsilon = \epsilon_+/\epsilon_-$.

It is to be expected that for any given values of $(\mathbf{r}, t)$ the resulting solution for F will be a good approximation if T is large enough. From (17′), it is seen that introducing the limit $T \to +\infty$ has the effect of removing from study the bremsstrahlung radiation produced while the charge accelerates from rest to its final velocity v. Thus by letting $T \to +\infty$ we are lead to a consideration of transition radiation not complicated by the presence of bremsstrahlung.

We note that f', as given in (17′), consists of two parts: a particular solution of (16) which corresponds to the field of the moving charge in an infinite homogeneous medium, and a homogeneous solution of (16) which arises because of the presence of the boundary.

Let us express f' as

$$f' = f_p' + f_h' \tag{20}$$

where f_p' is the particular solution to (16) and f_h' is the homogeneous solution to (16) in the limit $T \to \infty$. Likewise

$$f = f_p + f_h \tag{21}$$

where f_p and f_h are the inverse transforms of f_p' and f_h' with respect to x. Similarly we write

$$F = F_p + F_h\,. \tag{22}$$

The term F_p is easily evaluated (see Appendix):

$$F_p = -\frac{Q}{2\pi}\arctan\left\{\frac{z - vt}{x[1 - (v/c_\pm)^2]^{1/2}}\right\} \quad \text{for} \quad c_\pm > v, \tag{23a}$$

$$F_p = \frac{Q}{2}\,\mathrm{sgn}\,(x) u\left(vt - z - |x|\left[\left(\frac{v}{c_\pm}\right)^2 - 1\right]^{1/2}\right) \quad \text{for} \quad v > c_\pm\,. \tag{23b}$$

In (23) $c_\pm = (\mu_\pm\epsilon_\pm)^{-\frac{1}{2}}$ and $u(x)$ is the unit step function. Equation (23b) shows clearly the Cerenkov wedge associated with a line charge moving with a velocity greater than the speed of light in the medium.

Let us now briefly consider the transition radiation problem for a line dipole moving with uniform velocity v in the z-direction. The dipole is assumed to be oriented in the direction of a unit vector $\mathbf{1}_0$. Let $\mathbf{1}_x$ and $\mathbf{1}_z$ be the vector components of $\mathbf{1}_0$ transverse and parallel to the z-axis. Thus $\mathbf{1}_0 = \mathbf{1}_x + \mathbf{1}_z$. The resulting charge density for the moving dipole is

$$n(\mathbf{r}, t) = p\{[\mathbf{1}_x + (1 - v^2/c^2)^{1/2}\mathbf{1}_z]\cdot\nabla\}\ \delta(x)\ \delta(z - vt) \tag{24}$$

where p is the dipole strength and c is the speed of light in vacuo. The term $(1 - v^2/c^2)^{1/2}$ is due to the relativistic Lorentz–Fitzgerald contraction of a length which is parallel to the direction of motion. One notes that

$$\{n\}_{\text{line dipole}} = \frac{p}{Q}\left\{\left[\mathbf{1}_x + \left(1 - \frac{v^2}{c^2}\right)^{1/2}\mathbf{1}_z\right]\cdot\nabla\right\}\{n\}_{\text{line charge}}\ . \tag{25}$$

From (25) and the linearity of Maxwell's equations it follows that

$$\{F\}_{\text{line dipole}} = \frac{p}{Q}\left\{\left[\mathbf{1}_x + \left(1 - \frac{v^2}{c^2}\right)^{1/2}\mathbf{1}_z\right]\cdot\nabla\right\}\{F\}_{\text{line charge}} \tag{26}$$

with the resulting field quantities defined as in (7) and (8). Thus the solution to the line dipole problem may be simply obtained from the solution to the line charge problem as indicated in (26).

IV. Inversion of transforms.

A. *General Considerations.* This part of the paper will be devoted to an exact evaluation of the fields $\mathbf{E}_h$ and H_h corresponding to F_h. From (17) and (15) we see that f_h is given by

$$f_h = \frac{1}{2\pi}\int_{-\infty}^{+\infty} A_\pm(\eta)\ \exp\ \{i\alpha_\pm\ |z| + i\eta x\}\ d\eta. \tag{27}$$

Utilizing Eqs. (7), (8) and (27) we have, after interchanging differentiation and integration

$$\mathbf{e}_h' = \frac{1}{\epsilon_\pm}\ (\mp i\alpha_\pm\mathbf{x}_0 + i\eta\mathbf{z}_0)f_h' \tag{28}$$

and

$$h_h' = -i\omega f_h'\ . \tag{29}$$

The basic idea is to manipulate Eq. (27) so as to obtain

$$\mathbf{e}_h = \int_{-\infty}^{+\infty} \mathbf{V}(t)\ \exp\ (-i\omega t)\ dt, \qquad h_h = \int_{-\infty}^{+\infty} W(t)\ \exp\ (-i\omega t)\ dt$$

whence $\mathbf{E}_h$ is equal to $\mathbf{V}(t)$ and H_h is equal to $W(t)$. The transition from (27) will be accomplished by contour deformations in the complex plane and by transformation of variables. The general program outlined above has been used by other authors (cf. [3]–[7]).

In the integral (27) the square roots are defined so that the integral converges, as shown below, for small loss (i.e. $\epsilon_\pm = \epsilon_\pm'' + i\delta$ and $0 < \delta \ll \epsilon_\pm''$). Figures 2 and 3 are used to define α_- and α_+ respectively for $z > 0$, while 3 and 2 apply respectively to α_- and α_+ for $z < 0$. Thus both α_- and α_+ have positive imaginary parts on the path integration (i.e. the Re (η) axis).

Following Felsen [3] we introduced the transformation

$$\eta = k_\pm \sin w, \qquad z \gtrless 0. \tag{30}$$

Defining $A_+'(w)$ and $A_-'(w)$ as

$$A_+'(w) = -\frac{Qc_-^2 \sin w}{2c_+}\left\{\frac{1}{\left[\left(\frac{1}{\sigma}\right) - \sin^2 w\right]^{1/2} - \frac{c_+}{v}} - \frac{\left[\left(\frac{1}{\sigma}\right) - \sin^2 w\right]^{1/2} + \frac{c_+}{\epsilon v}}{\cos^2 w - \frac{c_+^2}{v^2}}\right\}$$
$$\div \left\{\cos w + \epsilon\left[\left(\frac{1}{\sigma}\right) - \sin^2 w\right]^{1/2}\right\}, \tag{31}$$

$$A_-'(w) = -\frac{Qc_- \sin w}{2}\left\{\frac{1}{[\sigma - \sin^2 w]^{1/2} + \frac{c_-}{v}} - \frac{[\sigma - \sin^2 w]^{1/2} - \frac{\epsilon c_-}{v}}{\cos^2 w - \frac{c_-^2}{v}}\right\}$$
$$\div \{[\sigma - \sin^2 w]^{1/2} + \epsilon \cos w\} \tag{32}$$

where $\sigma = (c_-/c_+)^2$, Eq. (27) becomes

$$f_h = \frac{1}{\pi}\int_P A_+'(w) \exp(irk_+ \cos(w - \theta)) \cos w \frac{k_+}{\omega^2}\, dw, \qquad z > 0, \tag{33}$$

$$f_h = \frac{1}{\pi}\int_P A_-'(w) \exp(irk_- \cos(w - \theta)) \cos w \frac{k_-}{\omega^2}\, dw, \qquad z < 0, \tag{34}$$

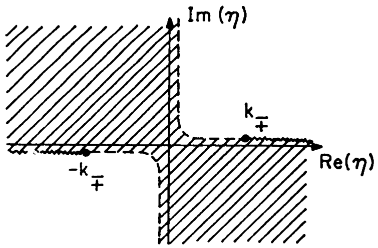

FIG. 2. Im $\alpha_\mp' > 0$ in the shaded region, and Re $\alpha_\mp' > 0$ on the top sheet.

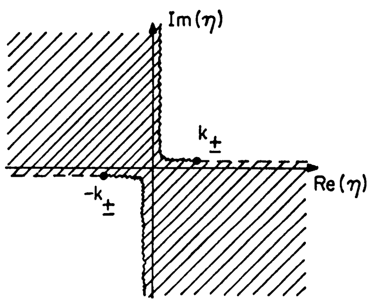

FIG. 3. Re $\alpha_\pm' > 0$ in the shaded region, and Im $\alpha_\pm' > 0$ on the top sheet.

where the variables r and θ have been introduced by setting

$$x = r \sin \theta \quad \text{and} \quad |z| = r \cos \theta.$$

The path of integration P is shown in Fig. 4. Note that F_h is an odd function of θ since $\theta \to -\theta$, $w \to -w$ leaves the integrand unchanged but reverses the direction of the path of integration.

Next the manner in which poles and branch points transform into the w-plane must be investigated. Depending on whether the parameters σ, v/c_+ and v/c_- are greater than or less than unity, the character of the disposition of poles and branch points will be basically different. Each case must be treated separately. In Table I all possible cases are listed. Cases 3 to 6 are distinguished by the presence of Cerenkov radiation. While these cases are quite interesting, it is not our purpose here to study the Cerenkov effect. Therefore we will concentrate on cases 1 and 2, which allow a study of transition radiation not complicated by the presence of Cerenkov radiation. Treatment of cases 3 to 6 is reserved for a future publication. Since the analysis and results are very similar for cases 1 and 2, only case 1 will be considered in detail. For case 1, $v < c_+ < c_-$. The disposition of poles[3] and branch points is shown in Figs. 5 and 6. In Figs. 5 and 6

$$w_{b_1} = \arc\sin \sigma^{-1/2}, \qquad w_{b_2} = \frac{\pi}{2} + i \operatorname{arc\,cosh} \sigma^{1/2}, \qquad w_{p_1} = i \operatorname{arc\,cosh} (c_+/v),$$

$$w_{p_2} = i \operatorname{arc\,cosh} (c_-/v),$$

$$w_{p_3} = i \operatorname{arc\,sinh} \{[(c_+/v)^2 - (c_+/c_-)^2]^{1/2}\}.$$

B. *Deformation of the Path of Integration.* The path of integration is now deformed to the straight line Re $(w) = \theta$. Care must be taken to avoid crossing any singularities. A typical situation is shown in Fig. 7.

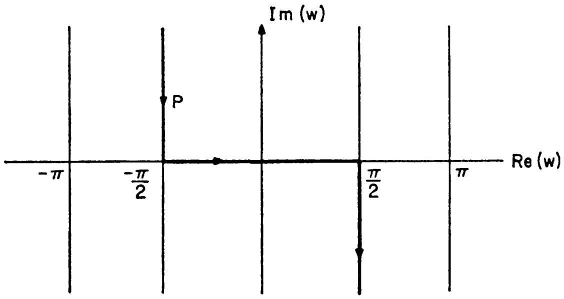

FIG. 4. Path of integration in the w-plane.

TABLE I: Parameter Ranges

case	σ	v/c_+	v/c_-
1	>1	<1	<1
2	<1	<1	<1
3	>1	>1	<1
4	<1	<1	>1
5	>1	>1	>1
6	<1	>1	>1

[3]Only poles on the top sheet of the w-plane are considered.

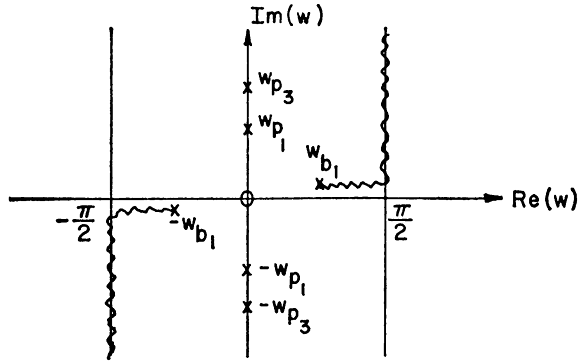

FIG. 5. Disposition of poles and branch points of the integrand in Eq. (33) for the case $v < c_+ < c_-$.

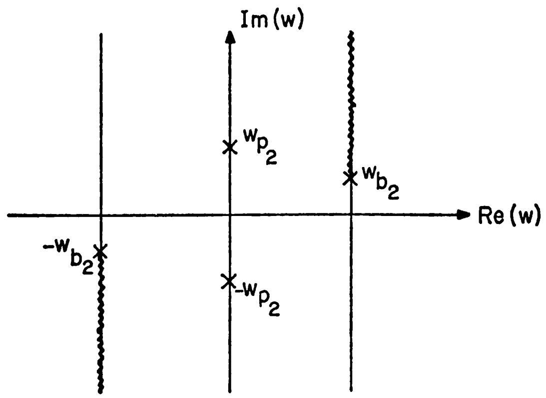

FIG. 6. Disposition of poles and branch points of the integrand in Eq. (34) for the case $v < c_+ < c_-$.

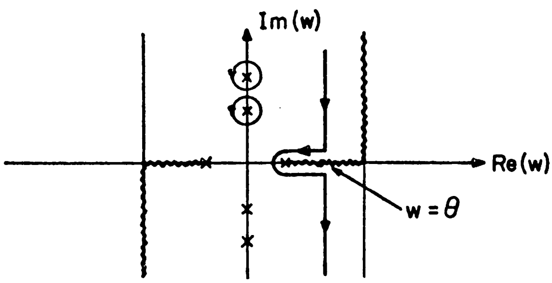

FIG. 7. New path of integration for Eq. (33) with $\theta > \arcsin(\sigma^{-1/2})$ and $v < c_+ < c_-$.

It may be shown [3] that the horizontal paths $i\infty - \pi/2$ to $i\infty + \theta$ and $-i\infty + \theta$ to $-i\infty + \pi/2$ do not contribute to the integral.

Thus f_h may be expressed as the sum of three terms

$$f_h = f^{(1)} + f^{(2)} + f^{(3)} \tag{35}$$

where

$f^{(1)}$ = the contribution to f_h from integration along $\mathrm{Re}(w) = \theta$,
$f^{(2)}$ = the contribution to f_h from integration around the branch cut,
$f^{(3)}$ = the contribution to f_h from integration around poles.

With the square roots defined as in Figs. 2 and 3 we have

$$A'_{\pm}(w^*) = [A'_{\pm}(w)]^*.$$

Thus the method of Felsen [3] is applicable, and $f^{(1)}$ may be inverted immediately.[4]

$$H^{(1)} = \frac{\partial F^{(1)}}{\partial t} = -\frac{2 \operatorname{Re} [A'_+(w_1) \cos w_1]}{\pi[(c_+t/r)^2 - 1]^{1/2}} \cdot \frac{u(c_+t - r)}{r} \quad \text{for} \quad z > 0, \tag{36}$$

$$H^{(1)} = \frac{\partial F^{(1)}}{\partial t} = -\frac{2 \operatorname{Re} [A'_-(w_2) \cos w_2]}{\pi[(c_-t/r)^2 - 1]^{1/2}} \cdot \frac{u(c_-t - r)}{r} \quad \text{for} \quad z < 0, \tag{37}$$

Likewise $\mathbf{E}^{(1)}$ for $z > 0$ is given by

$$\mathbf{E}^{(1)} = \frac{2 \operatorname{Re} [(-\cos w_1 \mathbf{x}_0 + \sin w_1 \mathbf{z}_0) A'_+(w_1) \cos w_1/c_+]}{\pi\epsilon_+[(c_+t/r)^2 - 1]^{1/2}} \cdot \frac{u(c_+t - r)}{r}, \tag{38}$$

and for $z < 0$

$$\mathbf{E}^{(1)} = \frac{2 \operatorname{Re} [(\cos w_2 \mathbf{x}_0 + \sin w_2 \mathbf{z}_0) A'_-(w_2) \cos w_2/c_-]}{\pi\epsilon_-[(c_-t/r)^2 - 1]^{1/2}} \cdot \frac{u(c_-t - r)}{r} \tag{39}$$

where $w_{1,2} = \theta - i \operatorname{arc\,cosh} (c_{\pm}t/r)$ and both $[(1/\sigma) - \sin^2 w_1]^{1/2}$ in (36) and $[\sigma - \sin^2 w_2]^{1/2}$ in (37) are defined so that they have positive real parts. Letting $\lambda_+ = c_+t/r$ in (36) and $\lambda_- = c_-t/r$ in (37) we obtain

$$F^{(1)} = \int_1^{\lambda_{\pm}} \frac{2 \operatorname{Re} [A'_{\pm}(w_{1,2}) \cos w_{1,2}/c_{\pm}]}{\pi(\lambda_{\pm}^2 - 1)^{1/2}} \, d\lambda_{\pm} \, u(\lambda_{\pm} - 1), \tag{40}$$

where $w_{1,2} = \theta - i \operatorname{arc\,cosh} \lambda_{\pm}$. Note that $F^{(1)}$ depends on r and t only through the variable t/r.

C. *Branch Cut Contribution.* For $z < 0$, $F^{(2)} = 0$. For $z > 0$, the branch point is intercepted when $|\theta| > \operatorname{arc\,sin} \sigma^{-1/2}$. Thus for $z > 0$ and $|\theta| < \operatorname{arc\,sin} \sigma^{-1/2}$, $F^{(2)} = 0$. Assuming $z > 0$ and $\pi/2 > \theta > \theta_c$ (where $\theta_c = \operatorname{arc\,sin} \sigma^{-1/2}$), $F^{(2)}$ is an integral along the path shown in Fig. 8, where δ is allowed to approach zero.
As $\delta \to 0$ the integral around the semicircle approaches zero. Thus

$$f^{(2)} = \lim_{\delta \to 0} \frac{k_+}{\pi} \left[\int_{\theta + i\delta}^{\theta_c + i\delta} \frac{1}{\omega^2} A'_+(w) e^{irk_+ \cos (w-\theta)} \cos w \, dw \right.$$
$$\left. + \int_{\theta_c - i\delta}^{\theta - i\delta} \frac{1}{\omega^2} \cos w A'_+(w) e^{irk_+ \cos (w-\theta)} \, dw \right]. \tag{41}$$

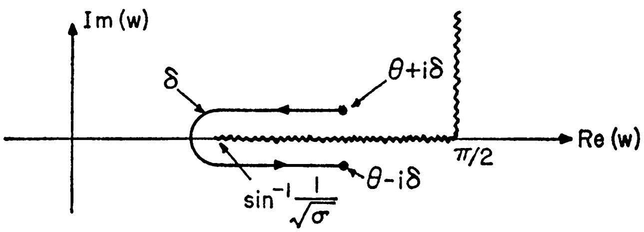

FIG. 8. $f^{(2)\prime}$ integration.

---

[4]Felsen accomplishes this by making a change of variables from w to t, $t = (r/c_{\pm}) \cos (w - \theta)$, thus reducing the integral along $\operatorname{Re}(w) = \theta$ to the desired form.

Since $A_+'(\alpha - i\delta) = [A_+'(\alpha + i\delta)]^*$,

$$f^{(3)} = \lim_{\delta \to 0} \frac{2ik_+}{\pi\omega^2} \int_{\theta_c - i\delta}^{\theta - i\delta} \cos w \operatorname{Im} [A_+'(w)] e^{irk_+ \cos (w-\theta)} \, dw. \tag{42}$$

In (42) we define a new variable of integration, t, by letting $c_+ t = r \cos (w - \theta)$. Equation (42) becomes

$$-i\omega f^{(3)} = \frac{-2}{c_+\pi} \int_{r/c_+ \cos (\theta_c - \theta)}^{r/c_+} \cos w_3 \operatorname{Im} A_+'(w_3) e^{i\omega t} \frac{c_+}{r \sin (w_3 - \theta)} \, dt, \tag{43}$$

where $w_3 = \theta + \operatorname{arc} \cos \lambda_+$, $\theta_c < w_3 < \pi/2$, and the square root in (43) is taken as

$$[(1/\sigma) - \sin^2 w_3]^{1/2} \equiv i[\sin^2 w_3 - 1/\sigma]^{1/2}.$$

Equation (43) is in the desired form and can be inverted by inspection:

$$H^{(2)} = \frac{\partial F^{(2)}}{\partial t} = -\frac{2 \cos w_3}{\pi r \sin (w_3 - \theta)} \operatorname{Im} A_+'(w_3) u(\theta - \theta_c)$$
$$\cdot u\left(t - \frac{r}{c_+} \cos [\theta_c - \theta]\right) u(z) u\left(\frac{r}{c_+} - t\right),$$

or

$$H^{(2)} = \frac{\partial F^{(2)}}{\partial t} = -\frac{2 \cos w_3}{\pi r (1 - \lambda_+^2)^{1/2}} \operatorname{Im} A_+'(w_3) u(1 - \lambda_+) u(z) u(w_3 - \theta) u(\theta - \theta_c). \tag{44}$$

So far only the case $\pi/2 > \theta > \theta_c$ has been considered. A similar consideration for $-(\pi/2) < \theta < -\theta_c$ shows that $F^{(2)}$ is an odd function of θ. Thus for the general case of $\pi/2 > |\theta| > \theta_c$

$$H^{(2)} = \frac{\partial F^{(2)}}{\partial t} = \frac{2 \cos w_3}{\pi r (1 - \lambda_+^2)^{1/2}} \operatorname{Im} A_+'(w_3) \operatorname{sgn} (\theta) u(1 - \lambda_+) u(z) u(w_3 - \theta_c) \tag{45}$$

where $w_3 = \operatorname{arc} \cos (\lambda_+) + |\theta|$, $\pi/2 > w_3 > \theta_c$, $\pi/2 > |\theta|$, and $[(1/\sigma) - \sin^2 w_3]^{1/2} = i[\sin^2 w_3 - 1/\sigma]^{1/2}$. Similarly we obtain for $\mathbf{E}^{(2)}$

$$\mathbf{E}^{(2)} = \frac{2 \cos w_3/c_+}{\pi r (1 - \lambda)^{1/2}} (\sin w_3 \mathbf{x}_0 - \cos w_3 \mathbf{y}_0)$$
$$\cdot \operatorname{Im} A_+'(w_3) \operatorname{sgn} (\theta) u(1 - \lambda_+) u(z) u(w_3 - \theta_c). \tag{46}$$

Thus from (45)

$$F^{(2)} = -\frac{2}{c_+\pi} \int_{\cos (\theta_c - |\theta|)}^{\lambda_+} \cos w_3$$
$$\cdot \operatorname{Im} A_+'(w_3) \frac{d\lambda_+}{(1 - \lambda_+^2)^{1/2}} \operatorname{sgn} \theta \cdot u(|\theta| - \theta_c) u(1 - \lambda_+) u(w_3 - \theta_c) u(z). \tag{47}$$

The final result is

$$F^{(2)} = \frac{2}{c_+\pi} \int_{\theta_c}^{w_3} \cos w_3 \operatorname{Im} A_+'(w_3) \, dw_3 \, u(1 - \lambda_+) u(w_3 - \theta_c) \operatorname{sgn} (\theta) u(|\theta| - \theta_c) u(z) \tag{48}$$

where $-(\pi/2) < \theta < \pi/2$,

$$w_3 = \operatorname{arc} \cos (\lambda_+) + |\theta|, \quad 0 < w_3 < \frac{\pi}{2}, \qquad [(1/\sigma) - \sin^2 w_3]^{1/2} = i[\sin^2 w_3 - 1/\sigma]^{1/2}.$$

Figure 9 shows the regions in space where $F^{(1)}$ and $F^{(2)}$ contribute. Evidently $F^{(1)} + F^{(2)}$ represents a burst of energy originating at the impact point. After impact this energy propagates outward from the impact point in the manner illustrated in Fig. 9.

From (48) we see that $F^{(2)}$ depends on the variables r, θ, t only through the single real variable $w_3 = [\text{arc cos } (c_+t/r) + |\theta|]$. Thus $F^{(2)}$ is constant along the lines $w_3 =$ constant. These curves are straight lines tangent to the wave front $r = c_+t$ as shown in Fig. 10. The variable w_3 itself has a simple geometric interpretation: it is the angle of the line from the origin to the point of tangency of the line of constant $F^{(2)}$. This is illustrated in Fig. 11.

The similarity properties of $F^{(1)}$ and $F^{(2)}$ (i.e. $F^{(1)}$ depends on r, θ, t only through t/r and θ, and $F^{(2)}$ is a function of w_3) may be inferred on other grounds [10], as was done by Gardner and Keller [8] and by Papadopoulos [9], who show that the lines $w_3 =$ constant are the characteristics of a certain hyperbolic equation.

What do the similarity properties of F imply for the physical field quantities $\mathbf{E}$ and $\mathbf{H}$? From Eq. (36) to (39) we readily infer that both $H_v^{(1)}$ and $\mathbf{E}^{(1)}$ have the functional form

$$g_1(t/r,\ \theta)/r.$$

From Eqs. (45) and (46), $H_v^{(2)}$ and $\mathbf{E}^{(2)}$ have the functional form

$$g_2(w_3)/r(1 - \lambda_+^2)^{1/2}.$$

The solution for case 2 of Table I may be obtained by letting $z \to -z$, $v \to -v$ and $c_\pm \to c_\mp$ in the expression for $F^{(2)}$. The equations for $F^{(1)}$ remain unchanged. For case 2 the regions where $F^{(1)}$ and $F^{(2)}$ contribute are the same as in Fig. 9 if one imagines the whole picture to be reflected across the x-axis.

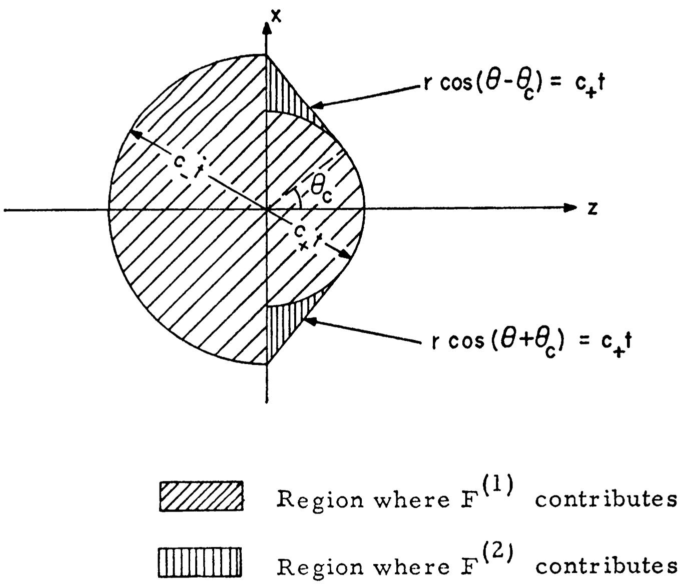

FIG. 9. Regions where $F^{(1)}$ and $F^{(2)}$ contribute.

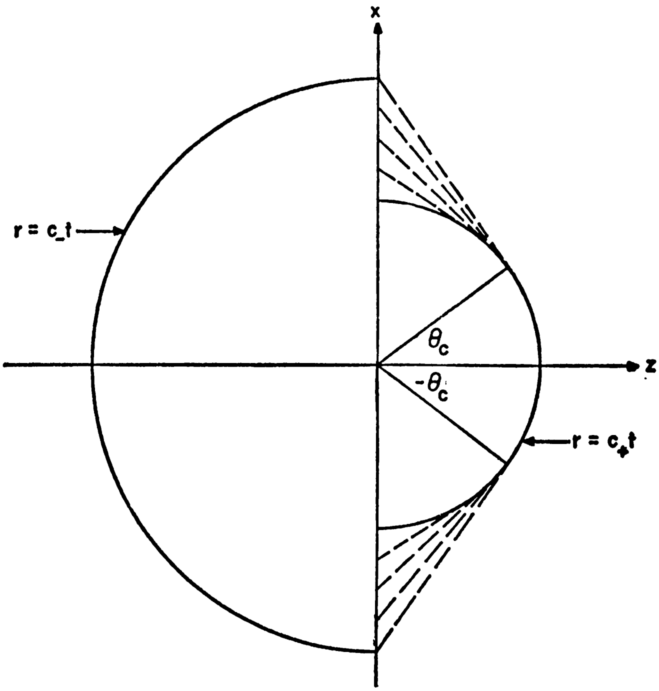

FIG. 10. $F^{(3)}$ constant along the dotted lines. The dotted lines are tangent to the circle $r = c_+t$.

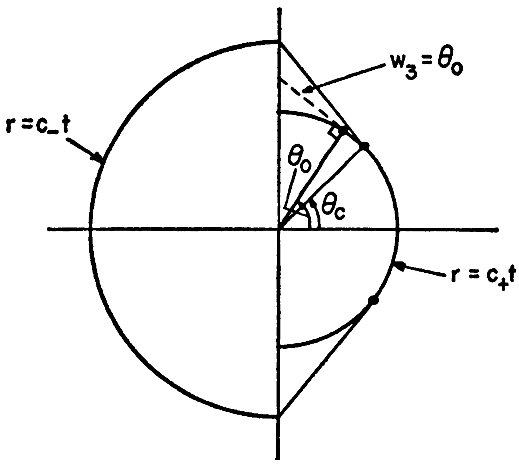

FIG. 11. The line $w_3 = \theta_0$.

D. *Pole Contributions.* We now evaluate $F^{(3)}$ for $z < 0$. We note from Fig. 6 that for $\theta > 0$ (i.e. $x > 0$) the pole at w_{p_3} is intercepted. This pole corresponds to

$$\eta = \eta_{p_3} = i\frac{\omega}{v}\operatorname{sgn}(\omega)(1 - \beta_-^2)^{1/2} \tag{49}$$

where $\beta_\pm = v/c_\pm$. At η_{p_3}

$$\alpha_+ = \frac{\omega}{v}(1 + \beta_+^2 - \beta_-^2)^{1/2} \tag{50}$$

and

$$\alpha_- = \omega/v. \tag{51}$$

Define

$$Z = \lim_{\eta \to \eta_{p_2}} [(\eta - \eta_{p_2}) A_-(\eta)] = \frac{Q}{2\omega} \cdot \frac{(1 + \beta_+^2 - \beta_-^2)^{1/2} - \epsilon}{(1 + \beta_+^2 - \beta_-^2)^{1/2} + \epsilon}. \tag{52}$$

Thus

$$f^{(3)} = iZ \exp\left\{-i\frac{\omega}{v} z - \frac{x}{v} |\omega| (1 - \beta_-^2)^{1/2}\right\}, \qquad x > 0. \tag{53}$$

Since F is an odd function of x

$$f^{(3)} = \frac{Q \operatorname{sgn}(x)}{2i\omega} \cdot \frac{\epsilon - (1 + \beta_+^2 - \beta_-^2)^{1/2}}{\epsilon + (1 + \beta_+^2 - \beta_-^2)^{1/2}} \exp\left\{-i\omega\frac{z}{v} - |\omega| \frac{|x|}{v} (1 - \beta_-^2)^{1/2}\right\} \tag{54}$$

for $z < 0$. Comparing $f^{(3)}$ with f_p for $v < c_-$ in the Appendix we have

$$F^{(3)} = -\frac{Q}{2\pi} \frac{(1 + \beta_+^2 - \beta_-^2)^{1/2} - \epsilon}{(1 + \beta_+^2 - \beta_-^2)^{1/2} + \epsilon} \arctan\left[\frac{z + vt}{x(1 - \beta_-^2)^{1/2}}\right], \qquad z < 0. \tag{55}$$

For $z > 0$ there are two poles, w_{p_1} and w_{p_2}. An analysis similar to that for $z < 0$ yields

$$F^{(3)} = \frac{Q}{2\pi}\left\{\arctan\left[\frac{z - vt}{x(1 - \beta_+^2)^{1/2}}\right] - \frac{2\epsilon}{\epsilon + (1 + \beta_+^2 - \beta_-^2)^{1/2}} \arctan\left[\frac{(1 + \beta_+^2 - \beta_-^2)^{1/2} z - vt}{x(1 - \beta_-^2)^{1/2}}\right]\right\} \tag{56}$$

for $z > 0$. Setting

$$Q_1 = \frac{(1 + \beta_+^2 - \beta_-^2)^{1/2} - \epsilon}{(1 + \beta_+^2 - \beta_-^2)^{1/2} + \epsilon} Q \tag{57}$$

$$Q_2 = \frac{2\epsilon}{(1 + \beta_+^2 - \beta_-^2)^{1/2} + \epsilon} Q \tag{58}$$

$$v_2 = v(1 + \beta_+^2 - \beta_-^2)^{-1/2} \tag{59}$$

we have

$$F_p + F^{(3)} = -\frac{Q}{2\pi} \arctan\left[\frac{z - vt}{x(1 - \beta_-^2)^{1/2}}\right] - \frac{Q_1}{2\pi} \arctan\left[\frac{z + vt}{x(1 - \beta_-^2)^{1/2}}\right] \tag{60}$$

for $z < 0$, and

$$F_p + F^{(3)} = -\frac{Q_2}{2\pi} \arctan\left[\frac{z - v_2 t}{x(1 - v_2^2/c_+^2)^{1/2}}\right] \quad \text{for} \quad z > 0. \tag{61}$$

With the fields $F_p + F^{(3)}$ represented as above we see that a simple image picture applies (cf. Figs. 12(a) and 12(b)).

The field created by the uniformly moving charges Q and Q_1 in the infinite homogeneous medium (ϵ_-, μ_-) in Fig. 12(a) is identical to $F_p + F^{(3)}$ when $z < 0$. Similarly, the uniformly moving charge Q_2 in Fig. 12(b) sets up a field identical to $F_p + F^{(3)}$ for $z > 0$.

For $t < 0$, $F^{(1)}$ and $F^{(2)}$ are zero. Thus the entire solution is given by the image pictures in Figs. 12(a) and 12(b). For $t > 0$, $F^{(1)}$ and $F^{(2)}$ are zero outside the cross-hatched regions in Fig. 9. Thus the image picture is again the entire solution in this region. Inside the cross-hatched regions (Fig. 9) the entire solution is the sum of the fields given by the images and $F^{(1)} + F^{(2)}$. For $t > 0$, Figs 13(a) and 13(b) show the resulting image picture.

For $t > 0$, there is one apparent objection to this solution. This is that image charges are located in the observation region (i.e. Q_1 is in the region $z < 0$ and Q_2 is in the region $z > 0$). Furthermore, the true charge Q in Fig. 13(b) does not appear in the observation region $z > 0$ where it is actually located. All these points may be clarified if one realizes that the field consists of the sum $(F_p + F^{(3)}) + F^{(1)} + F^{(2)}$. It may be shown that $\mathbf{E}^{(1)}$ has a singularity at $z = v_2 t$ which exactly cancels the singularity in $\mathbf{E}^{(3)}$ due to Q_2; also, $\mathbf{E}^{(1)}$ has a singularity at $z = vt$ which is the same as would be produced by a charge Q at that point.

The result that the image picture remains valid for $t > 0$ at observation points outside the domain of influence of $F^{(1)} + F^{(2)}$ may be explained as follows: at a time $t < 0$ an observer sees the field due to the image, which he assumes is due to an actual charge in an infinite homogeneous space. In fact, the observer has no way of knowing that the space is not infinite and that the image is not really a true charge. At $t = 0$ the charge strikes the boundary and the information that the space is not infinite begins to be felt. This information, however, is not immediately given to the observer but takes a finite amount of time to reach him. In fact, the information is contained within the domain of influence of $F^{(1)} + F^{(2)}$. As far as the observer is concerned, before the information reaches him the fields will be correctly given by the image picture.

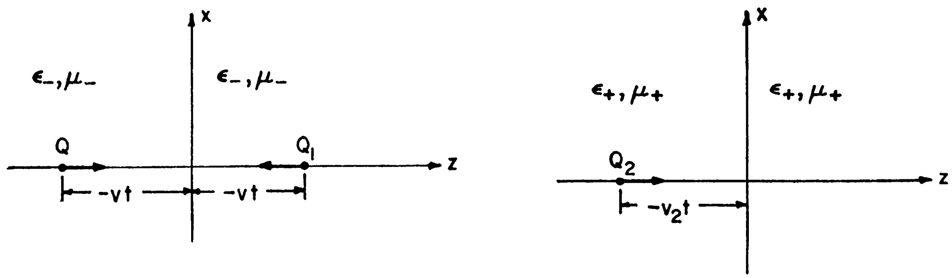

FIG. 12(a). Image picture for $z < 0$, $t < 0$.

FIG. 12(b). Image picture for $z > 0$, $t < 0$.

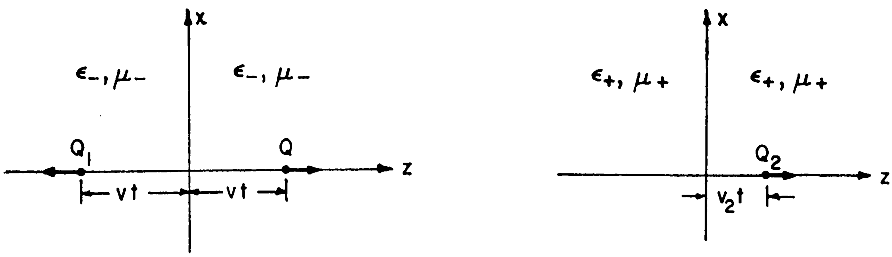

FIG. 13(a). Image picture applying for $z < 0$, $t > 0$.

FIG. 13(b). Image picture applying for $z > 0$, $t > 0$.

V. Further discussion of the solution.

A. *Nonrelativistic Approximation.* In order to obtain a nonrelativistic approximation to the fields, let $\gamma \to \infty$ in Eqs. (18) and (19). Then

$$A_+^\dagger = A_-^\dagger = -\frac{\eta v Q}{\omega^2} \cdot \frac{1-\epsilon}{\alpha_+ + \epsilon\alpha_-} \tag{62}$$

where the dagger means "nonrelativistic approximation to." Consider now the field of a pulsed line dipole slightly to the right of the interface (Fig. 1). The current density is

$$\mathbf{J} = J\ \delta(x)\ \delta(z - 0^+)u(t)\mathbf{z}_0 \tag{63}$$

where 0^+ denotes a small positive quantity and $u(t)$ is the unit step function. For this problem one may again define a scalar function F_d from which $\mathbf{E}$ and H_y may be found as before from Eqs. (7) and (8). Taking Fourier transforms in x and t and solving the resulting problem for f_d yields

$$f_d = B \exp(-i\alpha_\pm |z|) \tag{64}$$

where

$$B = -\frac{J\eta}{\omega^2} \cdot \frac{1}{\alpha_+ + \epsilon\alpha_-}. \tag{65}$$

Comparing Eqs. (62) and (65) we see that if

$$J = Qv(1 - \epsilon), \tag{66}$$

then

$$f_h^\dagger = f_d\ . \tag{67}$$

Thus Eq. (66) gives the strength of an equivalent current element which produces the same fields as the nonrelativistic transition radiation from a line charge of strength Q.

When is the approximation valid? Referring to Eqs. (44), (36) and (37), we see that the approximation is valid for[5]

(1) $c_\pm \gg v\ |\cos w_{1,2}|$ in the region where $F^{(1)}$ contributes,
(2) $c_+ \gg v\ |\cos w_3|$ in the region where $F^{(2)}$ contributes.

Since $\cos w_{1,2} = \cos[\theta - i \text{ arc cosh } \lambda_\pm] = \lambda_\pm \cos\theta + i(\lambda_\pm^2 - 1)^{1/2} \sin\theta$ and w_3 is real (thus $\cos w_3 \leq 1$), conditions (1) and (2) become

(1) $r \gg vt$
(2) $v \ll c_\pm$.

Clearly (1) breaks down if the observer is too close to the origin. Condition (1) will, however, be fulfilled over a very large percentage of the region where $F^{(1)}$ contributes (i.e., the region $c_\pm t \geq r$) if $c_\pm \gg v$. It is on this basis that the term "nonrelativistic" is justified. Figure 14 shows a graph of the percent error in the nonrelativistic approximation for H_h in the case $\epsilon \to \infty$, $\theta = 45°$. We note that for $v/c_- = 0.05$ the error is less than 2% for $r \geq c_-t/2$. For $v/c_- = 0.01$ the error is less than 1.25% for $r \geq c_-t/5$. This helps give some quantitative meaning to the requirement $r \gg vt$.

---

[5]It is assumed that neither ϵ nor $1/\epsilon$ is very large compared to unity.

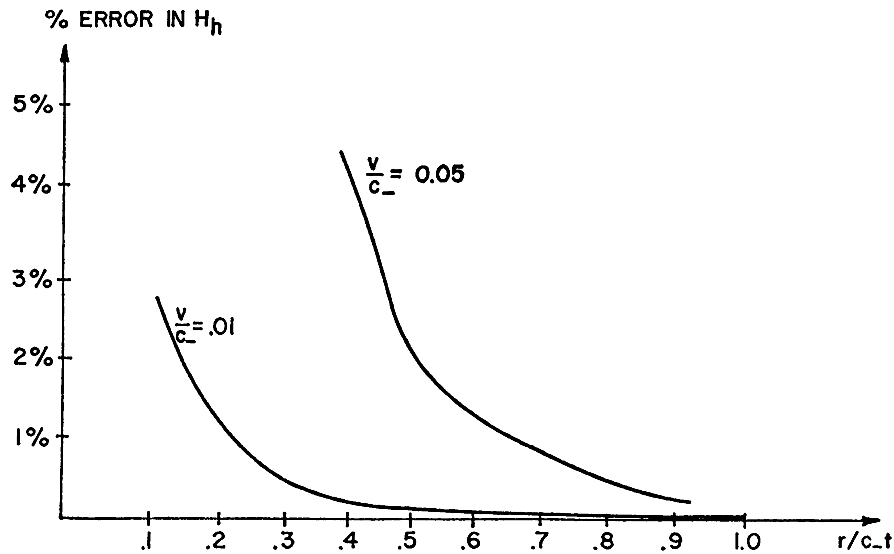

FIG. 14. % error in nonrelativistic approximation for $\epsilon \to \infty$, $\theta = 45°$, $z < 0$.

B. *Fields Near the Wavefronts.* We note that the solution possesses wavefronts at which it may be discontinuous or singular. These are the cylindrical wavefronts at $r = c_\pm t$ and the plane wavefront at $w_3 = \theta_c$. In this section we will be interested in the behavior of the fields near the wavefronts.

Near $r = c_\pm t$ we may approximate $w_{1,2}$ and $(c_\pm^2 t^2 - r^2)^{1/2}$ as

$$w_{1,2} = \theta - i \operatorname{arc\,cosh} (c_\pm t/r) \cong \theta, \tag{68}$$

$$(c_\pm^2 t^2 - r^2)^{1/2} \cong [2r(c_\pm t - r)]^{1/2} = (2rL_1)^{1/2} \tag{69}$$

where L_1 denotes the distance from the observation point to the wavefront, $r = c_\pm t$. Thus for $r \cong c_\pm t$

$$H^{(1)} \cong -\frac{2^{1/2}}{\pi} \cdot \frac{\operatorname{Re} [\cos \theta A_\pm'(\theta)]}{(rL_1)^{1/2}} u(c_\pm t - r). \tag{70}$$

Thus we see that $H^{(1)}$ diverges like $(L_1)^{-1/2}$ near the wavefront. Furthermore the strength of this singularity decreases as $(r)^{-1/2}$.

It is slightly more difficult to obtain an expression for $H^{(2)}$ near $w_3 = \theta_c$. For $w_3 \cong \theta_c$ the square root, $(1/\sigma - \sin^2 w_3)^{1/2}$, is a small positive imaginary quantity

$$i\delta = (1/\sigma - \sin^2 w_3)^{1/2}.$$

Thus,

$$A_+'(w_3) \cong -\frac{ac_-^2 \sin \theta_c}{2c_+} \left[\frac{1}{i\delta - c_+/v} - \frac{i\delta + c_+/(\epsilon v)}{\cos^2 \theta_c - c^2/v^2} \right] \div [\cos \theta_c + \epsilon i \delta]. \tag{71}$$

Expanding (71) for small δ yields

$$\operatorname{Im} \{A_+'(w_3)\} \cong -\frac{a\epsilon}{2c_+} \delta \left\{ \frac{v\epsilon c_-}{\epsilon - 1} \left[1 - \frac{1}{\epsilon - (\epsilon - 1)v^2/c_+^2} \right] \right.$$
$$\left. - \frac{\epsilon v^2/c_+^2}{(\epsilon^2 - \epsilon)^{1/2}} \left[1 - \frac{\epsilon}{\epsilon - (\epsilon - 1)v^2/c_+^2} \right] \right\} \tag{72}$$

where we have set $\sigma = \epsilon$ (i.e. $\mu_+ = \mu_-$) in order to simplify the algebra. It now remains to find an approximate expression for δ

$$\delta = (\sin^2 w_3 - 1/\sigma)^{1/2} \cong (2 \sin \theta_c)^{1/2}(\sin w_3 - \sin \theta_c)^{1/2}. \tag{73}$$

Near $w_3 = \theta_c$

$$\sin w_3 \cong \sin \theta_c + \sin (w_3 - \theta_c) \cos \theta_c . \tag{74}$$

Now to find $\sin (w_3 - \theta_c)$ (cf. Fig. 15). For B very close to C, B' is close to A' and we have

$$\sin (w_3 - \theta_c) \cong L_2/\overline{CA'} \tag{75}$$

where L_2 denotes the distance from the observation point to the wavefront. But

$$\overline{CA'} = r \sin (\theta - \theta_c) \tag{76}$$

and

$$L_2 = c_+t - r \cos (\theta - \theta_c). \tag{77}$$

Thus from Eqs. (73) to (77)

$$\delta \cong \left(\frac{2}{\epsilon}\right)^{1/2}(\epsilon - 1)^{1/4}\left[\frac{c_+t - r \cos (\theta - \theta_c)}{r \sin (\theta - \theta_c)}\right]^{1/2}. \tag{78}$$

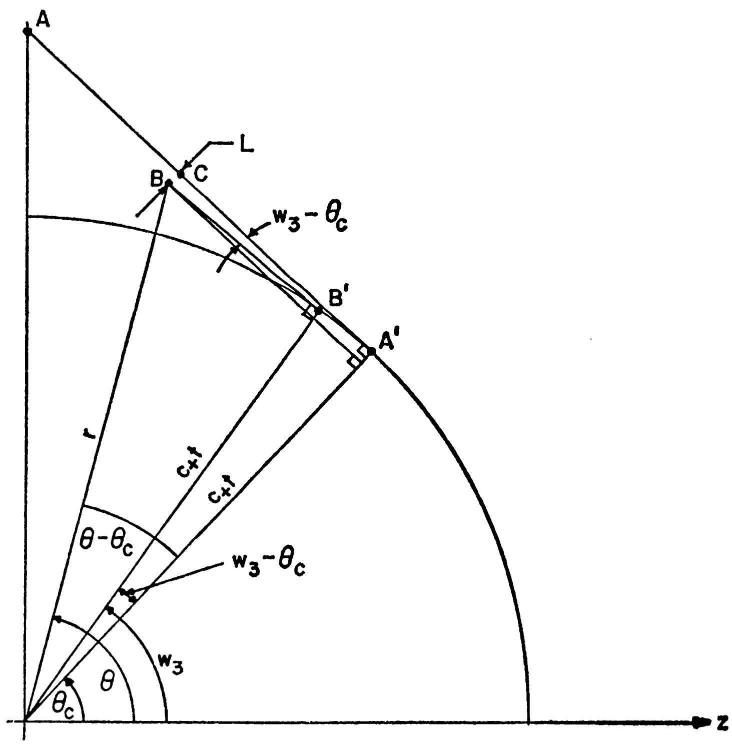

FIG. 15. Determination of $\sin (w_3 - \theta_c)$.

This approximation is valid as long as $L_2 \ll \overline{CA'}$. From Eqs. (44), (72) and (78) we obtain as the final result

$$H^{(2)} \cong K \frac{(L_2)^{1/2}}{(r \sin (\theta - \theta_c))^{3/2}} \tag{79}$$

where the constant K is given by

$$K = \frac{Q}{\pi c_+} (\epsilon - 1)^{3/4} \left(\frac{2}{\epsilon}\right)^{1/2} \left\{ \frac{v \epsilon c_-}{\epsilon - 1} \left[1 - \frac{1}{\epsilon - (\epsilon - 1) v^2 / c_+^2} \right] - \frac{v^2}{(\epsilon - 1)^{1/2}} \left[1 - \frac{\epsilon}{\epsilon - (\epsilon - 1) v^2 / c_+^2} \right] \right\},$$

for $\mu_+ = \mu_-$. Thus we see that H_y is continuous across $w_3 = \theta_c$ but that its first derivative is infinite at $w_3 = \theta_c$. We note that the behavior of H_y near the cylindrical wavefronts is much more singular than near the plane wavefronts.

It is well known that in a transient problem, such as the one we are treating, the wavefront discontinuities and singularities propagate according to the laws of geometrical optics [11], [12]. This is readily confirmed by Eqs. (70) and (79). $H^{(1)}$ has the $(r)^{-1/2}$ dependence typical of a geometrical optics cylindrical wave. This factor results from an application of energy conservation within a ray tube diverging from the origin. Since $r \sin (\theta - \theta_c)$ in Eq. (79) is a length along $w_3 = \theta$, $H^{(2)}$ is in the form of an inhomogeneous plane wave. Thus $H^{(2)}$ also obeys the laws of geometrical optics near the wavefront.

VI. Summary. An exact closed form solution for the transition radiation of a uniformly moving line charge has been obtained. This solution may be thought of as consisting of two parts. One part is essentially given by an image representation. The other part originates at the impact point and propagates outward.

Certain features of the solution have been discussed:

(1) its similarity properties,
(2) its behavior near the wavefronts,
(3) its behavior in the non-relativistic case.

The motion of the charge has been assumed normal to the interface and slow enough so that no Cerenkov radiation is produced. The authors have also treated the more general case of oblique incidence of the charge accompanied by Cerenkov radiation. The results of this investigation will be published in the near future.

Acknowledgement. This research was supported by the Office of Naval Research, Washington, D.C. under Contract No. NONR 839(38), ARPA Order No. 529.

This work will be submitted by Edward Ott to the faculty of the Polytechnic Institute of Brooklyn in partial fulfillment of the requirements for the degree of Doctor of Philosophy (Electrophysics).

Appendix: Evaluation of F_p. The object of this appendix is to derive Eq. (26). The subscripts $+$ and $-$ will be dropped here.

$$F_p = \frac{Q}{4\pi^2} \int_{-\infty}^{+\infty} \int_{-\infty}^{+\infty} \frac{\exp [i(\omega z/v + \eta x - \omega t)]}{\eta^2 - \omega^2(1/c^2 - 1/v^2)} \frac{i\eta}{i\omega} \, d\eta \, d\omega$$

or

$$F_p = \frac{1}{2\pi} \int_{-\infty}^{+\infty} f_p \exp(-i\omega t)\, d\omega$$

where for $v > c$

$$f_p = \frac{Q}{2\omega\pi} \int_{-\infty}^{+\infty} \eta \frac{\exp[i(\omega z/v + \eta x)]}{\eta^2 - K^2}\, d\eta \quad \text{with} \quad K = \omega\left[\left(\frac{1}{c^2}\right) - \left(\frac{1}{v^2}\right)\right]^{1/2}$$

and for $c > v$

$$f_p = \frac{Q}{2\omega\pi} \int_{-\infty}^{+\infty} \eta \frac{\exp[i(\omega z/v + \eta x)]}{\eta^2 + L^2}\, d\eta \quad \text{with} \quad L = \omega\left[\left(\frac{1}{v^2}\right) - \left(\frac{1}{c^2}\right)\right]^{1/2}$$

Case I: $v > c$. The poles of the integrand are displayed in Fig. A-1 for $\omega > 0$. Adding slight loss means giving the dielectric constant a small positive imaginary part. Thus for $\omega > 0$ the quantity K/ω has a small negative imaginary part. This allows us to define the path of integration so that the radiation condition is satisfied. The path of integration is shown in Fig. A-2. If $x < 0$ we close the integration path with a large semicircle at infinity in the lower half of the η-plane. The addition of this semicircular path leaves the value of the integral unchanged since the integrand goes exponentially to zero for $|\eta| \to \infty$ in the lower half η-plane. Applying the Cauchy residue theorem, it is seen that the value of the integral is $2\pi i$ multiplied by the residue at the pole $\eta = -K$. The result is

$$f_p = \frac{Q}{2i\omega} \exp\left[i\left(\frac{\omega}{v} z + Kx\right)\right] \quad \text{for} \quad x < 0.$$

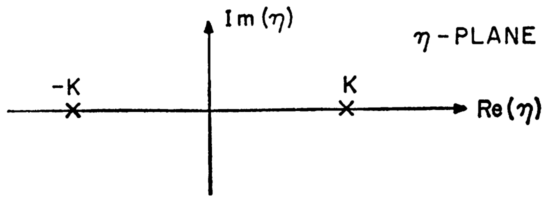

FIG. A-1. Poles.

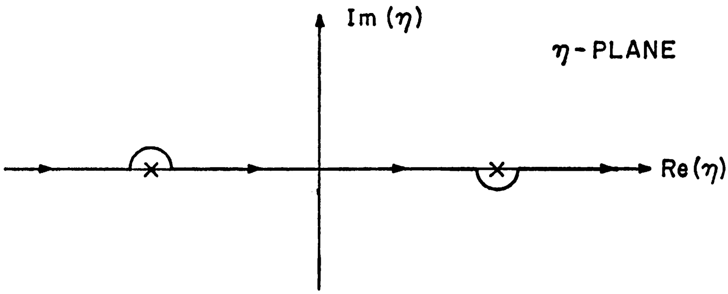

FIG. A-2. Integration path.

Likewise if $x > 0$ we can close the path in the upper half η-plane. We obtain

$$f_p = -\frac{Q}{2i\omega} \exp\left[i\left(\frac{\omega}{v} z - Kx\right)\right] \quad \text{for} \quad x > 0.$$

In both cases

$$f_p = -\frac{Q}{2i\omega} \operatorname{sgn}(x) \exp\left[i\left(\frac{\omega}{v} + K\,|x|\right)\right].$$

It turns out that the same result is obtained when it is assumed that $\omega < 0$. The inverse Fourier transform of f_p is

$$F_p = \frac{Q}{2} \operatorname{sgn}(x) u\left\{t - \frac{z}{v} - |x| \left[\left(\frac{1}{c^2}\right) - \left(\frac{1}{v^2}\right)\right]^{1/2}\right\}.$$

The behavior of F_p is illustrated in Fig. A-3.

Case II: $c > v$. In this case the poles of the integrand lie on the imaginary axis, and the integration path runs along the real axis (cf. Fig. A-4).

Closing the contour as before for $x > 0$ and $x < 0$ we obtain

$$f_p = \frac{-Q}{2i\omega} \operatorname{sgn}(x) \exp\left\{i\left(\frac{\omega z}{v}\right) - \omega\,|x| \left[\left(\frac{1}{v^2}\right) - \left(\frac{1}{c^2}\right)\right]^{1/2}\right\} \quad \text{for} \quad \omega > 0,$$

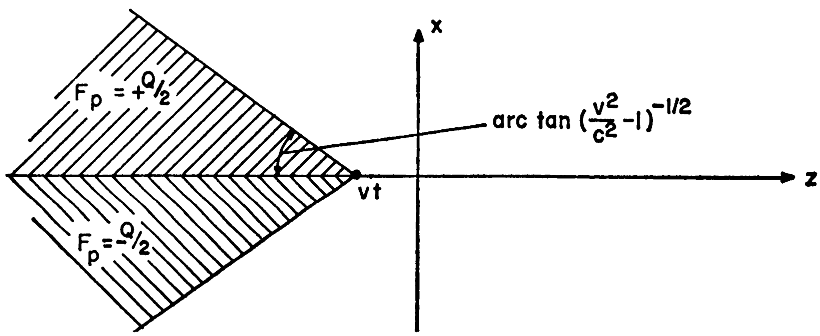

FIG. A-3. Cerenkov wedge.

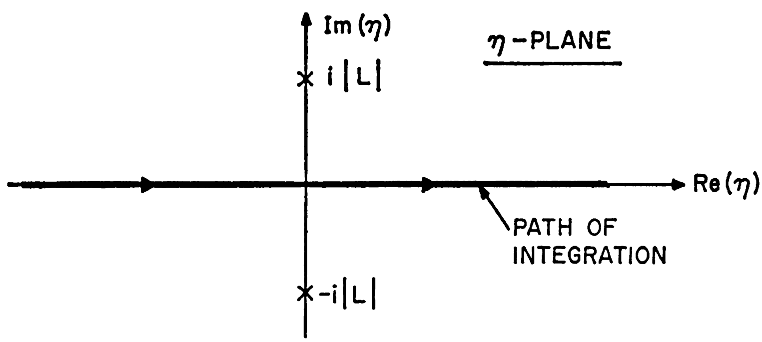

FIG. A-4. Integration path.

$$= \frac{-Q}{2i\omega} \operatorname{sgn}(x) \exp\left\{i\left(\frac{\omega z}{v}\right) + \omega\,|x| \left[\left(\frac{1}{v^2}\right) - \left(\frac{1}{c^2}\right)\right]^{1/2}\right\} \quad \text{for} \quad \omega < 0.$$

Thus

$$F_p = \frac{\operatorname{sgn}(x)}{4\pi}\left[\int_0^\infty \frac{-Q}{i\omega} \exp\left\{i\left(\frac{\omega z}{v}\right) - \omega\,|x| \left[\left(\frac{1}{v^2}\right) - \left(\frac{1}{c^2}\right)\right]^{1/2} - i\omega t\right\} d\omega\right.$$
$$\left. + \int_{-\infty}^0 \frac{-Q}{i\omega} \exp\left\{i\left(\frac{\omega z}{v}\right) + \omega\,|x| \left[\left(\frac{1}{v^2}\right) - \left(\frac{1}{c^2}\right)\right]^{1/2} - i\omega t\right\} d\omega\right].$$

Hence

$$F_p = \frac{i\operatorname{sgn}(x)}{2\pi}\int_0^\infty \frac{-Q}{i\omega} \sin\left[\omega\left(\frac{z}{v} - t\right)\right] \exp\left\{-\omega\,|x| \left[\left(\frac{1}{v^2}\right) - \left(\frac{1}{c^2}\right)\right]^{1/2}\right\} d\omega.$$

Let

$$\Omega = \omega\,|x|\,[(1/v^2) - (1/c^2)]^{1/2},$$

and

$$K' = \frac{(z/v) - t}{|x|\,[1 - (v/c)^2]^{1/2}}.$$

Then

$$F_p = -\frac{Q}{2\pi}\operatorname{sgn}(x)\int_0^\infty \frac{e^{-\Omega}}{\Omega}\sin(\Omega K')\,d\Omega.$$

But

$$\int_0^\infty \frac{e^{-\Omega}}{\Omega}\sin(\Omega K')\,d\Omega = \arctan K',$$

so that

$$F_p = -\frac{Q}{2\pi}\arctan\left\{\frac{z - vt}{x[1 - (v/c)^2]^{1/2}}\right\}.$$

References

[1] F. G. Bass and V. M. Yakovenko, *Theory of radiation from a charge passing through an electrically inhomogeneous medium*, Soviet Physics Uspekhi **8**, 420 (1965). [This is an extensive review article dealing with theoretical work on transition radiation.]

[2] I. M. Frank, *Transition radiation and optical properties of matter*, Soviet Physics Uspekhi **8**, 729 (1966). [This is a review article dealing with experimental work on transition radiation.]

[3] L. B. Felsen, *Transient solutions for a class of diffraction problems*, Microwave Research Institute, Polytechnic Institute of Brooklyn, Report PIBMRI-1209-64; also in Quart. Appl. Math. **23**, 151 (1965)

[4] B. Van der Pol and A. H. M. Levelt, *On the propagation of a discontinuous electromagnetic wave*, Proc. Acad. Sci. Amst. **A63**, 254 (1960)

[5] C. L. Pekeris and Z. Alterman, *Radiation resulting from an impulsive current in a vertical antenna placed on a dielectric ground*, J. App. Physics **28**, 1317 (1957)

[6] L. Cagniard, *Reflection and refraction of progressive seismic waves*, translated by E. Flinn and C. H. Dix, McGraw-Hill, New York, 1962. [This book is based on a series of papers published by Cagniard in the 1930's.]

[7] A. L. de Hoop, *Representation theorems for the displacement in an elastic solid and their application to elastodynamic diffraction theory*, Dissertation, University of Delft, The Netherlands, 1958
[8] C. S. Gardner and J. B. Keller, *The field of a pulsed dipole in an interface*, Comm. Pure Applied Math. **15**, 99 (1962)
[9] V. M. Papadopoulos, *A line source on an interface between two media*, Scientific Report AF 4561/5, Division of Engineering, Brown University, 1959; also in J. Fluid Mech. **8**, 41 (1960)
[10] E. Ott and J. Shmoys, *Transient fields created by a charge crossing a boundary between dielectrics*, Polytechnic Institute of Brooklyn, Report PIBMRI-1312-66, March, 1966
[11] F. G. Friedlander, *Sound pulses*, Cambridge Univ. Press, New York, 1958
[12] M. Kline and I. W. Kay, *Electromagnetic theory and geometrical optics*, Interscience, New York, 1966